

Aerial Diffusion: Text Guided Ground-to-Aerial View Translation from a Single Image using Diffusion Models

Divya Kothandaraman, Tianyi Zhou, Ming Lin, Dinesh Manocha
University of Maryland College Park

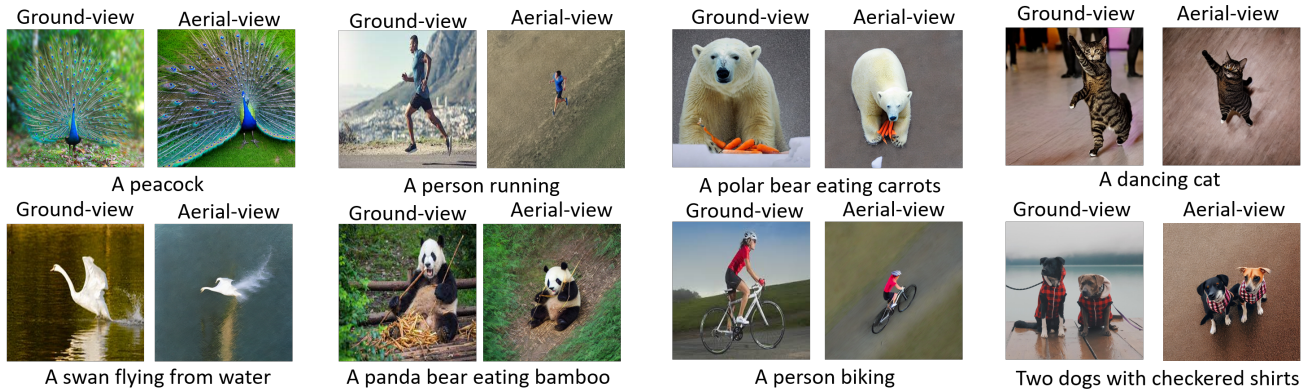


Figure 1: Given a single ground-view image and the corresponding text description as input, Aerial Diffusion generates corresponding aerial-view image. Our method does not require any supervision from aerial-view data, pairs of ground-aerial view, depth maps, semantic maps, multi-views, etc. It is one of the first approaches to achieve ground-to-aerial view translation in an unsupervised manner.

Abstract

We present a novel method, Aerial Diffusion, for generating aerial views from a single ground-view image using text guidance. Aerial Diffusion leverages a pretrained text-image diffusion model for prior knowledge. We address two main challenges corresponding to domain gap between the ground-view and the aerial view and the two views being far apart in the text-image embedding manifold. Our approach uses a homography inspired by inverse perspective mapping prior to finetuning the pretrained diffusion model. Additionally, using the text corresponding to the ground-view to finetune the model helps us capture the details in the ground-view image at a relatively low bias towards the ground-view image. Aerial Diffusion uses an alternating sampling strategy to compute the optimal solution on complex high-dimensional manifold and generate a high-fidelity (w.r.t. ground view) aerial image. We demonstrate the quality and versatility of Aerial Diffusion on a plethora of images from various domains including nature, human actions, indoor scenes, etc. We qualitatively prove the effectiveness of our method with extensive ablations and comparisons. To the

best of our knowledge, Aerial Diffusion is the first approach that performs single image ground-to-aerial translation in an unsupervised manner. Code is available at <https://github.com/divyakraman/AerialDiffusion>.

1. Introduction

The analysis of aerial image and video [35] plays a pivotal role in different applications, such as search and rescue, aerial photography, surveillance, movie production, etc. However, the paucity of aerial data [38] and the complexities associated with data capture from aerial cameras/UAVs makes it difficult and costly to train large neural networks [85] for these applications. Hence, the synthesis of aerial-view images [5] offers a promising alternative to address these challenges. Conditional image synthesis [47, 50] allows for control over the generation process.

Ground-view annotated datasets [12, 9, 7, 48] are readily available for many tasks. Hence, a method that transforms ground-view images to aerial views (or cross-view synthesis [55, 73]) could allow the reuse of annotated metadata for a variety of aerial-view applications, e.g., clas-

sification [22], segmentation [21], action recognition [34], representation learning [71], domain adaptation [8], augmentation [30], etc. However, cross-view synthesis requires the network to learn a very large non-trivial translation. The network needs to hallucinate a new and enormously different view of all entities in the scene and the background, while being consistent with the details including the semantics, colors, relations between various parts of the scene, pose, etc.

Prior work [55, 73, 14, 42] on ground-to-aerial generation use NeRFs and GANs. However, all of these methods use paired data for ground-view and the corresponding aerial views, which is seldom available. Moreover, training on a specific dataset limits the application to specific scenes similar to the training data; necessitating the collection of paired data for widely different distributions. Instead, our goal is to develop a generic method for generating aerial views from ground-views without any paired data or other auxiliary information such as multi-views, depth, 3D mapping, etc.

While there are many diverse datasets of ground images, there are not many such good quality aerial datasets [38] - hence, unpaired image-to-image translation [90] is not a viable solution. On the contrary, text is an auxiliary modality that can be easily obtained using off-the-shelf image/video captioning tools [25]. Moreover, text provides a natural representation space describing images. Consequently, our goal is to use the text description of a ground-view image to generate its corresponding aerial view.

Recently, diffusion models have emerged as state-of-the-art architectures for text-to-image [32, 23, 88, 50] high-quality realistic image synthesis. The availability of immense prior knowledge via large-scale robust pretrained text-to-image models [58], motivates us to pose ground-to-aerial view translation as text-guided single-image translation [32, 88]. Text-guided single-image translation methods finetune the diffusion model to the input image and then perform linear interpolation in the text embedding space to generate the desired output. However, direct application of these methods [50, 88, 32] to ground-to-aerial translation either generates high-fidelity non-aerial images or low-fidelity aerial images.

Main contributions. We present two postulates for text-guided image translation, for ground-to-aerial translation: (i) domain gap between the finetuning task (w.r.t. ground view) and target task (aerial view generation) hinders the diffusion model from generating accurate target views and introduces bias towards the source view, (ii) a finetuned diffusion model cannot generalize well to the target prompt, if the text embedding and image spaces corresponding to the source and the target are far apart on the nonlinear text-image manifold.

Based on these findings, we propose “*Aerial Diffusion*”, a simple, yet effective, method for generating aerial views, given a single ground-view image and the corresponding text

description as input. The novel elements of our algorithm include:

- Instead of directly finetuning the diffusion model with the ground-view image, we apply a *homography based on inverse perspective mapping* on the ground-view image to obtain a homography projected image prior to the finetuning. This reduces the bias of the diffusion model towards the input image while finetuning.
- To finetune the diffusion model, we use the *source text* corresponding to the ‘ground-view’ as the *guiding factor*, instead of the target text (‘aerial view’). This helps the diffusion model search for an optimized text embedding in the vicinity of a text space close to the image space, enabling the learning of a ‘good’ optimized text embedding. This also prevents the diffusion model from developing a bias towards an incorrect aerial view.
- To obtain a high-fidelity aerial image (w.r.t. ground-view), at inference time, we manipulate the text embedding layer, such that it prioritizes fidelity and the aerial viewpoint in an alternating manner. *Alternating between text embeddings corresponding to the viewpoint and fidelity switches the denoising direction*, such that the backward diffusion takes one step towards preserving fidelity followed by another step towards generating an aerial view. As noises are gradually removed, the process ends up with a high-fidelity aerial-view image on a manifold with a better fidelity-viewpoint trade-off than linear interpolation.

We apply our method on numerous in-the-wild images from various domains such as nature, animals and birds, human actions, indoor objects, etc. Our method is able to generate high-quality aerial view images that preserve the details contained in the source-view image (Fig. 2 and Fig. 1). We conduct extensive ablation studies (Fig. 7) highlighting the benefits of each element of our method; and demonstrate the trade-off between fidelity (w.r.t. source image) and faithfulness to target view via hyperparameter tuning (Fig. 5). We compare with the state-of-the-art diffusion model-based text-guided editing approach [32] and show far superior qualitative performance for ground-to-aerial translation (Fig. 7). Comparison to other text-embedding manipulation approaches (Fig. 7) also shows that our alternate prompting strategy works better.

2. Related work

There has been immense work on *image-to-image translation* [29, 43, 39, 51, 90, 79, 1] using GANs [64], transformers [15], diffusion models [13, 58, 10], etc. for problems, such as style transfer [31], image restoration [69], and multimodal style translation [28]. Many of these methods are capable of performing these tasks using paired/unpaired data [2]. Recently, diffusion models [50, 78, 70, 62, 60, 61, 84, 53] have been successful in performing

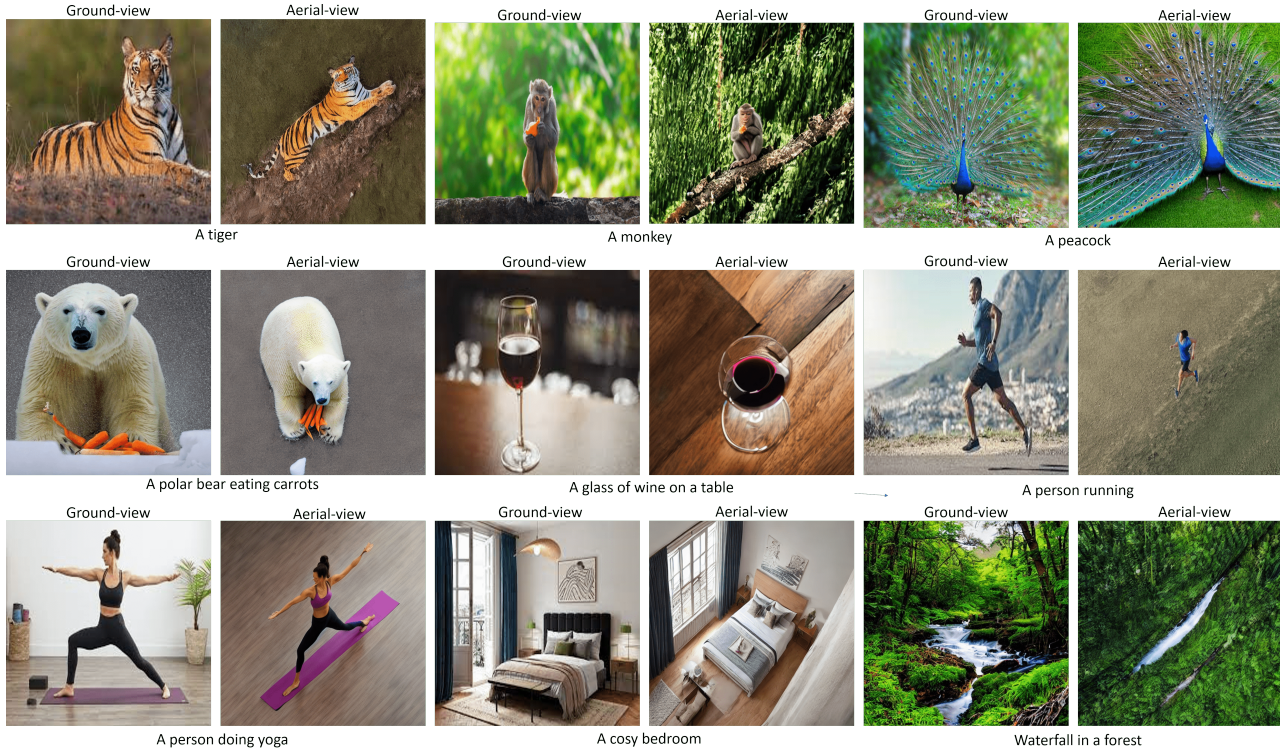


Figure 2: **Results.** We apply Aerial Diffusion on diverse images such as animals/ birds, natural scenes, human actions, indoor settings, etc and show that our method is able to generate high-quality high-fidelity aerial images.

non-trivial operations, such as posture changes and multiple objects editing. Prior work on *cross-view synthesis* [55, 73, 57, 74, 14, 45, 42, 67, 41, 56, 40, 82, 66, 3, 89] generally use paired data and other complex auxiliary modality such as semantic maps, depth, multi-views, etc within various generative approaches.

A closely related problem is *novel view synthesis* [36, 49] where the goal is to generate new views of the scene. However, most novel-view synthesis methods including GANs [83], NeRFs [19], diffusion models [80] use multiple views of the scene for training, even while they may be capable of performing single-view evaluation [81, 75]. Again, this is prohibitive since it requires multiple views of the scene/ depth information [26] for training. On the other hand, 3D reconstruction methods [20, 87, 16] rely on depth information or auxiliary data such as shape priors. Moreover, 3D reconstruction is a complex and expensive task, which is redundant when the goal is to just obtain a 2D aerial view of the scene.

Text, which is easily available, has been widely used as a guiding factor for image translation [44, 37] and image editing [32, 23, 6, 33, 88, 91, 27, 18, 11], particularly in the context of diffusion models recently. The availability of large databases of image-text pairs [63], open-source pretrained models [54], and the fact that text is a natural

representation of the world makes it conducive to use text as an auxiliary modality to provide guidance. Many *text-based image editing* approaches operate on a single real image [76, 32] and perform inference time optimization, making them easy to generalize across diverse images. *Single-image approaches* [86, 77, 59] have been proposed for image manipulation tasks without text-guidance as well. Generally, they aim to learn useful representations by finetuning a pretrained model on a single image for reconstruction. The inference then controls the feature space [65, 52] to achieve the desired changes.

3. Aerial Diffusion

We present Aerial Diffusion for view translation from a single real ground-view source image I_S to its aerial-view (or target image I_T), given a text description txt of the image. The text description can be obtained using an off-the-shelf image captioning tool [25]. We assume no access to any paired data or other modalities such as depth, semantic maps, other views of the scene, etc. Corresponding to the ground-view, we use the source text description $\text{txt}_G = \text{'front view of'} + \text{txt}$ with text embedding e_{src} . Similarly, for the aerial-view, we use the target text description $\text{txt}_A = \text{'aerial view of'} + \text{txt}$ with text embedding e_{tgt} . In Section 3.1, we present two

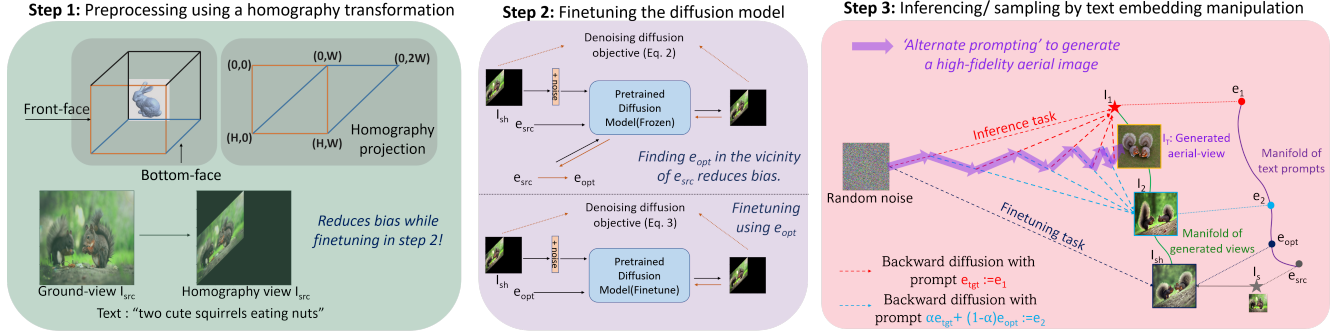


Figure 3: **Aerial Diffusion.** In step 1, we apply a homography transformation to the ground-view image I_S . This creates a gap between I_{Sh} and txt, which in turn reduces the bias of the model towards I_{Sh} in step 2. In step 2, we use the e_{src} to optimize to e_{opt} and finetune the diffusion model to reconstruct I_{Sh} for the e_{opt} . Using the e_{src} to find e_{opt} reduces the bias of the model towards I_{Sh} due to the disparity between I_{Sh} and the e_{src} . In stage 3, we manipulate the text embedding by using an alternating strategy to find the optimal solution in a higher-dimensional non-linear space to generate a high-fidelity aerial image I_T .

postulates that lead to the method described in Section 3.2.

3.1. Postulates

In this section, we analyze text-guided single image translation in the context of ground-to-aerial view synthesis and present two postulates. A common strategy adopted for text-based single image translation is to use a robust text-to-image pretrained model in a two-stage process. The first step finds the ‘optimized text embedding’ e_{opt} (in the vicinity of e_{tgt}) that best generates the ‘source’ image I_S and subsequently finetune the diffusion model to generate the ‘source’ image I_S using e_{opt} . In the second step, a linear interpolation of e_{tgt} and e_{opt} are used to generate the edited image I_T from the finetuned neural network, i.e., the backward diffusion process is

$$x_{t-1} = x_t - f(x_t, t, \alpha e_{tgt} + (1-\alpha)e_{opt}), t = T, \dots, 0. \quad (1)$$

A text-based single image translation approach [32, 23, 6, 33] for ground-to-aerial generation overcomes multiple limitations in terms of data availability and generalization. However, the challenges involved in ground-to-aerial translation inhibit the direct application of existing text-based single image translation methods for ground-to-aerial generation. We present two postulates for text-based single-image translation in the context of ground-to-aerial generation.

Postulate 3.1. *Domain gap between the finetuning task (e.g., ground view generation) and target task (aerial view generation) hinders the diffusion model from generating accurate target views and introduces bias towards the source view.*

Diffusion models are probabilistic models. They are trained [24] by optimizing the negative log-likelihood of the model distribution under the expectation of the data distribution. Further simplification of the equation for formulating

the training loss function involves variance reduction. In the first step of finetuning, the diffusion model is being trained to reproduce the source image given the optimized text embedding, irrespective of the input random noise. Hence, it has a natural bias towards the source image.

When the image space corresponding to the target text embedding is in the vicinity of the image space corresponding to the optimized text embedding, consistent with the variance within which the neural network was trained to generate, the generated target image is a high fidelity image consistent with the target text. When the desired transformation is large (ground-to-aerial), outside the limits of the variance, the diffusion model is unable to generate an aerial image.

Postulate 3.2. *A finetuned diffusion model cannot generalize well to the target prompt if the text embedding and image spaces corresponding to the source and the target are very different and far away from each other on the nonlinear text-image embedding manifold.*

The embedding space and the corresponding image representation space are locally linear. Hence, when the target text embedding dictates a relatively small change to the source image, a linear combination between the optimized text embedding and the target text embedding generates a high-fidelity target image, faithful to the target text. In contrast, when a linear interpolation of the text prompts in Eq. (1) is applied to ground-to-aerial translation, depending on α , the images generated are either high fidelity (but low target text faithfulness) or high target text faithfulness (but low fidelity). Moreover, the ground-view image doesn’t gradually change to an oblique-view image followed by aerial-view image, the manifold is not smooth. Rather, the change is quite drastic and it is difficult to find an optimal solution in the linear inter-

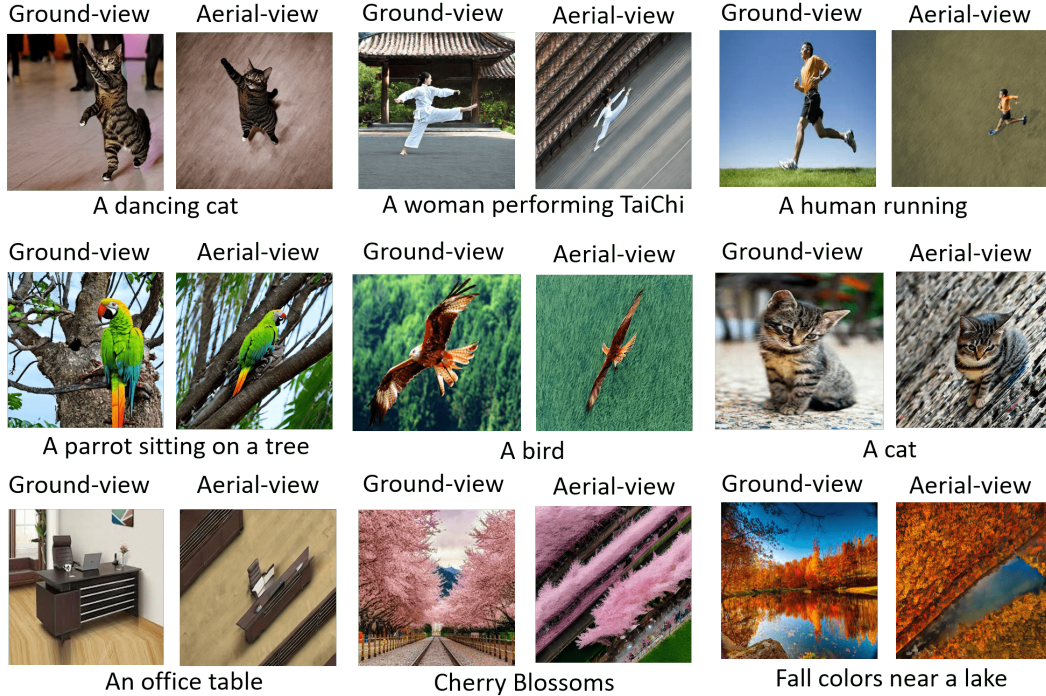


Figure 4: **Results.** We apply Aerial Diffusion on diverse images such as animals/ birds, natural scenes, human actions, indoor settings, etc and show that our method is able to generate high-quality high-fidelity aerial images.

polarization space. Essentially, when there is a large perspective changes from the source to target images (i.e. involving large rotation of camera poses), the image representation space is no longer “locally linear”, thereby linear interpolation is no longer adequate to generate high-fidelity images.

3.2. Method

Motivated by the challenges described above, we propose Aerial Diffusion for text guided single-image ground-to-aerial translation. An overview of our solution is as follows. We start with a pretrained robust stable diffusion [58] model as the backbone. Our method has three stages. In the first step, we preprocess the ground-view image I_S with a carefully crafted homography transformation to generate I_{Sh} . This reduces the bias in the finetuning step. In the second step, we finetune the diffusion model by first optimizing the text-embedding within the vicinity of e_{src} to find e_{opt} that best generates I_{Sh} . Subsequently, we finetune the diffusion model to reconstruct I_{Sh} , given e_{opt} . In the third step on inferring/sampling, we use an alternating strategy to manipulate the text embedding layer to generate a high-fidelity aerial image I_T . Next we describe each step in detail.

Step 1: Preprocessing using a homography transformation. The bias acquired by the diffusion model during the second step of finetuning inhibits large transformations. One

way to decrease the bias is to reduce the number of iterations while finetuning. However, this leads to unsurprisingly low quality generated images. To decrease the bias while finetuning, we preprocess the ground-view image by transforming it with a 2D *homography transformation* [72] (inverse perspective mapping). This homography projects the ground-view image to its rough 2D projected aerial view. Note that we are unable to use a 3D homography mapping to obtain the 3D aerial view projection, a better pseudo estimate of the aerial view, due to the unavailability of camera matrix, multi-views, depth information, etc. On the other hand, depth estimation methods [17, ?] increase the complexity of the problem.

Consider a 3D cube (Figure 3). Without loss of generality, the 2D image captured by a ground-camera can be regarded as the projection of the scene in the front-face of the cube. A camera facing the top face of the cube will be able to capture the accurate 2D aerial view of the scene. Since we have no knowledge of the camera parameters corresponding to the ground-view image, we are unable to shift the camera to obtain a different view of the scene. With respect to the ground-camera, the 2D projection of the front-face of the cube on the bottom face of the cube is the best ‘aerial projection’ that we can get (inverse perspective mapping [72]). This aerial projection is nowhere close to the true aerial view and does not resemble the ground-view either. Hence, when the diffusion model is finetuned, the bias is much lower than

what it would have been if the optimization/finetuning were done directly with the ground-view image. This is because of the disparities between the image space of I_{Sh} and e_{src}/e_{tgt} , ingrained in the pretrained network. Moreover, it provides a pseudo estimate of the direction in which the image needs to be transformed in order to generate its aerial view at the inference stage.

We maintain the horizontal and vertical distance between the edges of the faces in the ground view and its projected aerial view, to better preserve the resolution and the aspect ratio. Formally, the coordinates (in order) of the corners of the ground-view image and the homography projected image are $\{(0, 0), (H, 0), (H, W), (0, W)\}$ and $\{(0, W), (H, 0), (H, W), (0, 2W)\}$ respectively (Figure 3). The homography can then be computed and applied.

Step 2: Finetuning the diffusion model. We first optimize the text-embedding [32, 88] to generate I_{Sh} and subsequently finetune the diffusion model using e_{opt} to generate I_{Sh} . In contrast to popular text-based image editing approaches that find the optimized text embedding e_{opt} in the vicinity of the target text embedding e_{tgt} , we find e_{opt} in the vicinity of the source text embedding e_{src} . This is due to two reasons: (i) the disparity between the homography transformed view and the target text is still large (though much smaller than the disparity between the ground-view and target text). Hence, it is unlikely that a good e_{opt} will be obtained when the optimization is run (around e_{tgt}) for a limited number of iterations. (ii) we do not want the network to develop a bias towards the homography image as the ‘aerial view’.

To find e_{opt} , we freeze the parameters of the generative diffusion model f_θ and optimize e_{src} using the denoising diffusion objective [24]. This optimization is run for a small number of iterations, in order to remain close to e_{src} for meaningful embedding space manipulation at inferencing.

$$\min_{e_{opt}} \sum_{t=T}^0 L(f(x_t, t, e_{opt}; \theta), I_{Sh}), \quad (2)$$

where $f(x, t, y)$ is the t -th backward diffusion step, θ denotes the U-net parameters, and L is the denoising diffusion objective. To enable e_{opt} reconstruct the I_{Sh} with high fidelity, we finetune the diffusion model, again using the denoising diffusion objective [24, 61, 32]:

$$\min_{e_{theta}} \sum_{t=T}^0 L(f(x_t, t, e_{opt}; \theta), I_{Sh}). \quad (3)$$

Step 3: Inferencing/ sampling by text embedding manipulation. Our next step is to use the finetuned diffusion model to generate a high-fidelity aerial image. Prior work [32, 88] use linear interpolation between the optimized text embedding e_{opt} and the target text embedding e_{tgt} . As described

in Section 3.1, linear interpolation is not the best solution for large transformations such as ground-to-aerial generation and is unable to generate high-fidelity aerial images.

Sampling from stable diffusion [58] involves iteratively denoising the image for T steps conditioned by text, starting with random noise. To deal with the aforementioned issues, we propose to alternate between two text embeddings e_1 and e_2 , starting with e_1 . We designate e_1 as the target text embedding e_{tgt} . This imposes a strong constraint on the diffusion model to generate an aerial view image corresponding to the text description. The bias of the diffusion neural network motivates the network to generate an image whose details are close to the ground-view image. However, merely relying on the bias of the neural network to capture all details of the scene is severely insufficient. Hence, we designate e_2 to be the linear interpolation of e_{opt} and e_{tgt} , controlled by the hyperparameter α . The linear interpolation can be mathematically represented as $e_2 = \alpha * e_{tgt} + (1 - \alpha) * e_{opt}$. e_2 enables the network to generate a high fidelity image while retaining the aerial viewpoint. For very low values of α , the generated image is less aerial, despite reinforcing the viewpoint to be aerial by applying e_1 alternately. This is because of the bias of the neural network. Very high values of α result in low fidelity images, some details of the generated aerial image are not consistent with the ground-view image. An optimal solution is by tuning α .

Linear interpolation enforces the generation of an image consistent with a text embedding in the linear space between e_{opt} and e_{tgt} . This is a reasonable when the desired change is small: when the image spaces corresponding to e_{opt} and e_{tgt} are closeby, linear interpolation works due to local linearity. When the desired change is large (such as ground-to-aerial translation), the image spaces corresponding to e_{opt} and e_{tgt} are not nearby. Since the representation spaces are not globally linear, it becomes essential to search for the solution in a much higher dimensional non-linear space. This is achieved by our alternating strategy. The pseudo code for the alternating strategy is given below.

Algorithm 1: Alternate Prompting in backward diffusion enables the diffusion model generate a high-fidelity aerial image

```

1  $x_T \sim \mathcal{N}(0, I)$ ;
2 for  $t \leftarrow T$  to 0 do
3   if  $t \% 2 = 0$  then
4      $x_{t-1} = x_t - f(x_t, t, \alpha e_{tgt} + (1 - \alpha) e_{opt})$ ;
5   else
6      $x_{t-1} = x_t - f(x_t, t, e_{tgt})$ ;

```

While the sampling repetitively alternates between e_1 and e_2 , it is more beneficial to use e_1 (over e_2) at the first iteration. When the diffusion process starts with e_1 , the network

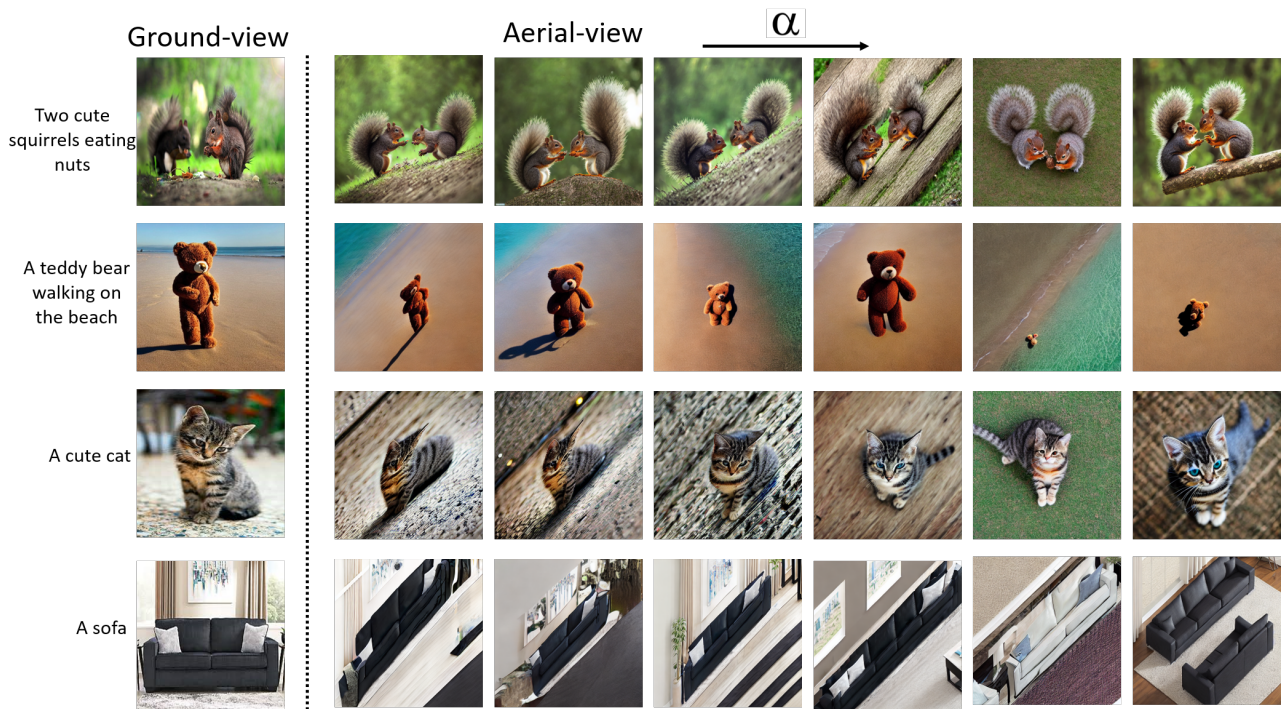


Figure 5: **Effect of α .** Low values of α generate images that are less aerial, high values of α generate low-fidelity images. A trade-off between the viewpoint and fidelity generates high-fidelity aerial images. The transformation, with α , is not smooth, reinforcing Postulate 2.

generates starts by generating an aerial image with details weakly dictated by its bias. Subsequent iterations that alternate between e_2 and e_1 fortify the generation of a high fidelity aerial image. On the contrary, when the diffusion process starts with e_2 , the generated image in the first iteration is less aerial though with very high fidelity. The bias, along with e_{opt} serve as a strong prior towards a non-aerial viewpoint. Subsequent iterations that use e_1 are unable to overcome this strong prior to alter the viewpoint to aerial view. Hence, we start inferencing with e_1 .

4. Experiments and Results

4.1. Implementation details

We use the stable diffusion [58] text-to-image model as the backbone architecture. It has been pretrained on the massive text-image LAION-5B dataset (laion2B-en, laion-high-resolution, laion-improved-aesthetics). Prior to the homography transformation, we resize all images to a resolution of 256×256 . We use OpenCV to apply the homography transformation on the image to generate a homography transformed image of resolution 512×512 , which is used to optimize the text embedding and the diffusion model in the next step. We finetune the text embedding for 500 iterations with a learning rate of $1e - 3$ using the Adam optimizer, and the diffusion model for 1000 iterations at a learning rate

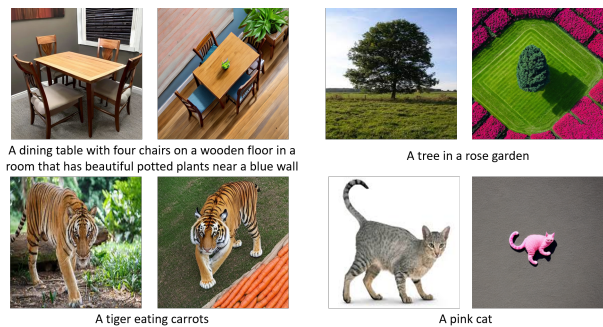


Figure 6: Based on the text description, Aerial Diffusion can generate aerial views with scene entities slightly different from the ground-view. The hallucination of background and unseen parts of the scene can also be controlled by text.

of $2e - 6$. For each image, this entire optimization takes between 8 and 9 minutes on one NVIDIA RTX A5000 GPU with 24GB memory.

While sampling/inferencing using the finetuned diffusion model, we iteratively refine the image, starting with random noise, for $T = 50$ iterations. At every iteration, the diffusion model is applied on the refined image from the previous iteration, as per the standard procedure [24] in sampling from diffusion models. The text embedding condition, while

sampling at each iteration, alternates between e_1 and e_2 , starting from e_1 . The guidance scale is set to 7.5.

4.2. Qualitative evaluation

We apply our method on a number of real images from various domains including nature, human actions, buildings, etc. We collect most of these images from Google Images/Flickr. We show the results in Figure 1 and Figure 2. Aerial images can be captured from varying heights and angles (including side/oblique views). We do not constrain the network on the height/ angle, hence, the diffusion model generates an aerial image of arbitrary height/ angle dictated by the random noise. For each image, we choose the best result corresponding to $0 < \alpha < 1$. Aerial Diffusion is successful in generating the aerial view, given its ground-view. It is able to hallucinate the aerial view of the entities in the scene (encompassing unseen aspects) as well as the background; while being faithful to the details in the ground-view. Since the underlying diffusion model is probabilistic, we get different results for different random seeds, all the generated images are faithful to the details in the ground-view as well as conform to the viewpoint being aerial. This diversity allows users to choose among a variety of options and is also a useful property in curating synthetic datasets.

More applications. We show in Figure 6 that our method is capable of generating aerial views consistent with the text description, even when the text dictates an aerial view with scene entities slightly different from the ground-view. Moreover, background hallucination can be controlled by the text description as well.

Effect of α . We show the effect of α in Figure 5. The finetuned diffusion model has high bias towards the ground-view image. Hence, the value of α needs to be carefully tuned in order to generate a high fidelity aerial image. A low value of α implies higher weight to the optimized text embedding and low weight to ‘aerial view’. This leads to the generated image being very similar to the homography image, the viewpoint of the generated image is less aerial. A high value of α implies higher weight to ‘aerial view’. The generated image is an aerial image, though with low fidelity. While the details in the generated aerial image are not completely different from the details in the ground-view image, due to the bias of the finetuned diffusion model, the fidelity or conformance to details contained in the ground-view image is still low. A good trade-off between fidelity w.r.t. ground-view image and ‘aerial view’ is achieved at mid-values of α . The change from ground-view to aerial-view as α varies from 0 to 1 is not gradual, reinforcing Postulate 2.

4.3. Ablations and comparisons

Ablating the model. We show ablation experiments in Figure 7. Ablation 1 uses the ground-view image instead of the homography transformed image to finetune the diffu-

sion model. It proves that the homography transformation is successful in significantly lowering the bias of the model and helps generate aerial views, reinforcing our solution to Postulate 1. Ablation 2 uses linear interpolation for sampling instead of our alternating strategy. Results with the alternating strategy are better (high fidelity images with faithfulness to ‘aerial view’) than the results with linear interpolation, justifying our solution to Postulate 2. Ablation 3 finds e_{opt} in the vicinity of e_{tgt} instead of e_{src} . Generated images are more aerial when e_{opt} is optimized in the vicinity of e_{src} , proving that it helps in reducing the bias.

SOTA Comparisons. We compare with IMAGIC [32] (CVPR 2023), DreamBooth [59] (CVPR 2023), SINE [88], SOTA text-based single image translation methods, in Figure 7, 14. Our method is far superior than prior art for ground-to-aerial translation, which are unable to effectively perform ground-to-aerial translation due to the high bias incurred while finetuning and searching for the solution in a limited linear interpolation space.

Comparisons with other text embedding manipulation methods. We compare with other strategies to manipulate the text embedding space using e_1 and e_2 in Figure 7. In manip1, we condition on e_2 and e_1 alternately, starting from e_1 . Clearly, it is more beneficial to start sampling from e_1 as explained in Section 3.2. In manip2, we use just e_1 (text embedding corresponding to aerial view) to sample and rely on the bias of the network to generate the aerial image. Our alternating sampling method is able to generate higher fidelity aerial images. In manip3, for the first $T/2$ iterations, we sample using e_1 and for the second $T/2$ iterations, we sample using e_2 . In manip4, for the first $T/2$ iterations, we sample using e_2 and for the second $T/2$ iterations, we sample using e_1 . These experiments prove that our alternating sampling strategy works best.

Quantitative evaluation - user study. Text guided single image ground-to-aerial translation is a recent development, and Aerial Diffusion is the first solution towards this goal. As such, no standard benchmark (and ground-truth) or quantitative metrics exist for evaluation. We evaluate Aerial Diffusion via human perceptual evaluation and observe that Aerial Diffusion is able to generate high-fidelity aerial images. We conduct the following types of evaluation:

1. **Image Quality:** Given a ground-view image and an aerial-view image generated using Aerial Diffusion, we ask participants to determine if the generated aerial-view image is a high-fidelity (w.r.t. ground-view image) aerial-view image; and rate the image on the 5-point Likert scale. The average rating over 10 images (rated by 49 participants) is 3.289.
2. **Alternating Sampling:** Given a ground-view image and two aerial-view images generated using Aerial Diffusion and Ablation 2 (i.e. Aerial Diffusion without the Alternating Sampling method) respectively, we ask par-

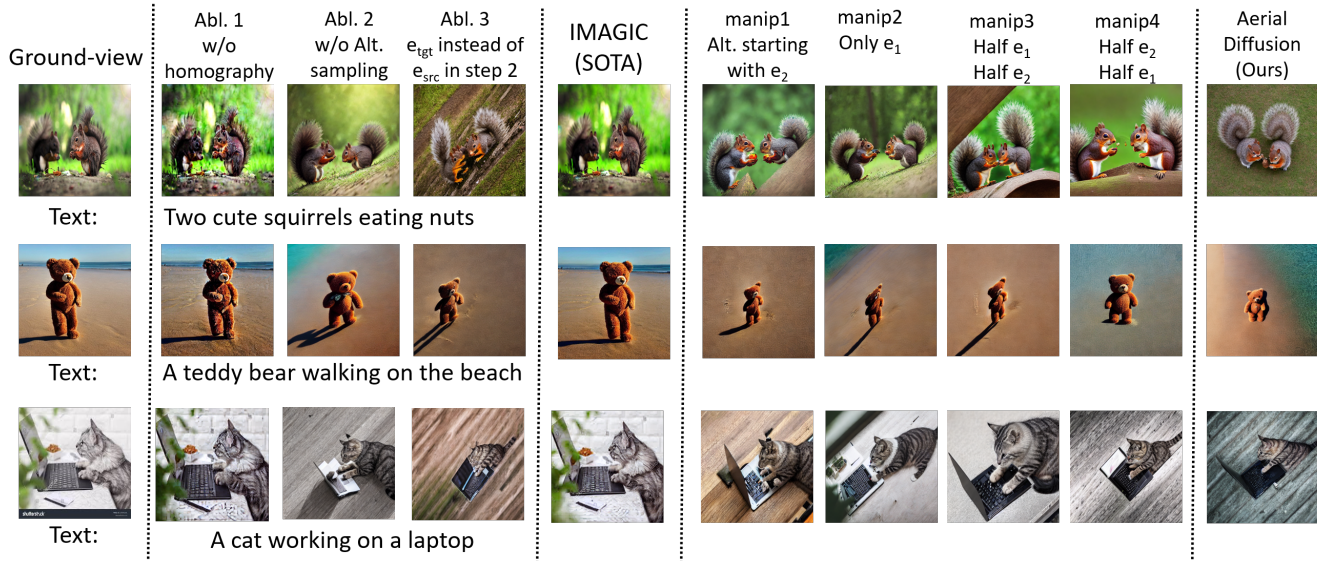


Figure 7: **Ablations and Comparisons.** Ablations: we prove the effectiveness of the homography, our alternating strategy over linear interpolation and finetuning with e_{src} instead of e_{tgt} . SOTA Comparisons: IMAGIC [32] (CVPR 2023) is unable to generate aerial views due to high bias towards the input image, domain gap and restricting the solution search to the linear interpolation manifold. Comparisons with other embedding space manipulation strategies that utilize both e_1 and e_2 reveal that our Alternating strategy is better.

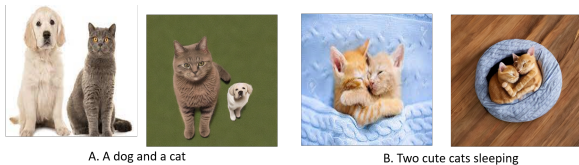


Figure 8: **Failure cases.** A. The identity of the dog and cat is interchanged. B. The fidelity of the background (bed) is lost.

Participants to choose the better high-fidelity aerial-view image. **83.05%** of the participants rate the image generated using Aerial Diffusion as the one with higher quality.

3. **Reference for Aerial Diffusion:** Given a ground-view image and two aerial-view images generated using Aerial Diffusion and Ablation 3 (Aerial Diffusion with e_{tgt} instead of e_{src} while training) respectively, we ask participants to choose the higher fidelity aerial-view image. **78.125%** of the participants rate the image generated using Aerial Diffusion as the one with higher quality.

Quantitative evaluation - metrics. Our method uses prior knowledge (from robust pretraining), along with the knowledge gained while finetuning, to generate aerial images. It *hallucinates* large parts and views of the scene that it has not encountered before. Hence, comparisons against other

ground-to-aerial methods [55, 74, 14, 66], that learn a specific data distribution by training on (an entire dataset with) paired data (and auxiliary information such as depth, semantic maps) is not relevant to this paper. In line with prior work [50, 88, 23, 32, 59] on text-based image translation, we report two metrics: (i) LPIPS to evaluate fidelity of aerial image w.r.t. ground-view image - the average score for 1 - LPIPS is 0.352 (higher, the better). However, similarity scores (such as FID, LPIPS) compute patch-wise image similarity and the aerial view is much different from the ground-view. No better evaluation strategy is available and is a direction for future work. (ii) CLIP score to evaluate the alignment of the generated aerial image with the text (dictating the viewpoint to be aerial) - the average CLIP score is 0.3233 (higher, the better). For reference, text-based image-editing methods such as Imagic [32] (CVPR 2023) and DreamBooth [59] (CVPR 2023) achieve CLIP scores of 0.25 to 0.3 on image editing dictating far lesser change than front-to-aerial translation.

More results. Please refer to the supplementary material.

5. Conclusion, Limitations and Future Work

In this paper, we introduce a novel method, Aerial Diffusion, for generating aerial views from a single ground-view image using text as a guiding factor. We use homography as guidance and a diffusion model on the generated image with an alternating denoising direction based on switching between viewpoint text embedding and fidelity of the gener-

ated images. Our method has some limitations. Our method has some limitations: (i) the homography transformation results in a directional (diagonal) bias in the generated aerial image in many cases; (ii) it is limited to the knowledge contained in the pretrained stable diffusion model and is unable to hallucinate scenes [68] outside of this domain; (iii) the value of α in sampling needs to be manually tuned; (iv) the problem domain of unpaired ground-to-aerial does not have concrete quantitative analysis metrics. Future work can focus on the development of methods that overcome these limitations. Other directions include extending Aerial Diffusion to complex scenes with multiple objects (and an intricate background), generating higher-fidelity images, extending the method to videos, using the synthetic aerial data for aerial video analysis, detection, and recognition tasks.

Acknowledgements: This research has been supported by ARO Grants W911NF2110026 and Army Cooperative Agreement W911NF2120076

References

- [1] Nuha Aldausari, Arcot Sowmya, Nadine Marcus, and Gelareh Mohammadi. Video generative adversarial networks: a review. *ACM Computing Surveys (CSUR)*, 55(2):1–25, 2022. 2
- [2] Aziz Alotaibi. Deep generative adversarial networks for image-to-image translation: A review. *Symmetry*, 12(10):1705, 2020. 2
- [3] Syed Ammar Abbas and Andrew Zisserman. A geometric approach to obtain a bird’s eye view from an image. In *Proceedings of the IEEE/CVF International Conference on Computer Vision Workshops*, pages 0–0, 2019. 3
- [4] Omer Bar-Tal, Dolev Ofri-Amar, Rafail Fridman, Yoni Kasten, and Tali Dekel. Text2live: Text-driven layered image and video editing. In *Computer Vision–ECCV 2022: 17th European Conference, Tel Aviv, Israel, October 23–27, 2022, Proceedings, Part XV*, pages 707–723. Springer, 2022. 15
- [5] Antonella Barisic, Frano Petric, and Stjepan Bogdan. Sim2air-synthetic aerial dataset for uav monitoring. *IEEE Robotics and Automation Letters*, 7(2):3757–3764, 2022. 1
- [6] Tim Brooks, Aleksander Holynski, and Alexei A Efros. Instructpix2pix: Learning to follow image editing instructions. *arXiv preprint arXiv:2211.09800*, 2022. 3, 4
- [7] Joao Carreira and Andrew Zisserman. Quo vadis, action recognition? a new model and the kinetics dataset. In *proceedings of the IEEE Conference on Computer Vision and Pattern Recognition*, pages 6299–6308, 2017. 1
- [8] Jinwoo Choi, Gaurav Sharma, Manmohan Chandraker, and Jia-Bin Huang. Unsupervised and semi-supervised domain adaptation for action recognition from drones. In *Proceedings of the IEEE/CVF Winter Conference on Applications of Computer Vision*, pages 1717–1726, 2020. 2
- [9] Marius Cordts, Mohamed Omran, Sebastian Ramos, Timo Rehfeld, Markus Enzweiler, Rodrigo Benenson, Uwe Franke, Stefan Roth, and Bernt Schiele. The cityscapes dataset for semantic urban scene understanding. In *Proceedings of the IEEE conference on computer vision and pattern recognition*, pages 3213–3223, 2016. 1
- [10] Florinel-Alin Croitoru, Vlad Hondru, Radu Tudor Ionescu, and Mubarak Shah. Diffusion models in vision: A survey. *arXiv preprint arXiv:2209.04747*, 2022. 2
- [11] Katherine Crowson, Stella Biderman, Daniel Kornis, Dashiell Stander, Eric Hallahan, Louis Castricato, and Edward Raff. Vqgan-clip: Open domain image generation and editing with natural language guidance. In *Computer Vision–ECCV 2022: 17th European Conference, Tel Aviv, Israel, October 23–27, 2022, Proceedings, Part XXXVII*, pages 88–105. Springer, 2022. 3
- [12] Jia Deng, Wei Dong, Richard Socher, Li-Jia Li, Kai Li, and Li Fei-Fei. Imagenet: A large-scale hierarchical image database. In *2009 IEEE conference on computer vision and pattern recognition*, pages 248–255. Ieee, 2009. 1
- [13] Prafulla Dhariwal and Alexander Nichol. Diffusion models beat gans on image synthesis. *Advances in Neural Information Processing Systems*, 34:8780–8794, 2021. 2
- [14] Hao Ding, Songsong Wu, Hao Tang, Fei Wu, Guangwei Gao, and Xiao-Yuan Jing. Cross-view image synthesis with deformable convolution and attention mechanism. In *Pattern Recognition and Computer Vision: Third Chinese Conference, PRCV 2020, Nanjing, China, October 16–18, 2020, Proceedings, Part I 3*, pages 386–397. Springer, 2020. 2, 3, 9
- [15] Patrick Esser, Robin Rombach, and Bjorn Ommer. Taming transformers for high-resolution image synthesis. In *Proceedings of the IEEE/CVF conference on computer vision and pattern recognition*, pages 12873–12883, 2021. 2
- [16] George Fahim, Khalid Amin, and Sameh Zarif. Single-view 3d reconstruction: A survey of deep learning methods. *Computers & Graphics*, 94:164–190, 2021. 3
- [17] Huan Fu, Mingming Gong, Chaohui Wang, Kayhan Batmanghelich, and Dacheng Tao. Deep ordinal regression network for monocular depth estimation. In *Proceedings of the IEEE conference on computer vision and pattern recognition*, pages 2002–2011, 2018. 5
- [18] Rinon Gal, Yuval Alaluf, Yuval Atzmon, Or Patashnik, Amit H Bermano, Gal Chechik, and Daniel Cohen-Or. An image is worth one word: Personalizing text-to-image generation using textual inversion. *arXiv preprint arXiv:2208.01618*, 2022. 3
- [19] Kyle Gao, Yina Gao, Hongjie He, Denning Lu, Linlin Xu, and Jonathan Li. Nerf: Neural radiance field in 3d vision, a comprehensive review. *arXiv preprint arXiv:2210.00379*, 2022. 3
- [20] Xian-Feng Han, Hamid Laga, and Mohammed Bennamoun. Image-based 3d object reconstruction: State-of-the-art and trends in the deep learning era. *IEEE transactions on pattern analysis and machine intelligence*, 43(5):1578–1604, 2019. 3
- [21] Shijie Hao, Yuan Zhou, and Yanrong Guo. A brief survey on semantic segmentation with deep learning. *Neurocomputing*, 406:302–321, 2020. 2
- [22] Zhengyu He. Deep learning in image classification: A survey report. In *2020 2nd International Conference on Information Technology and Computer Application (ITCA)*, pages 174–177. IEEE, 2020. 2
- [23] Amir Hertz, Ron Mokady, Jay Tenenbaum, Kfir Aberman, Yael Pritch, and Daniel Cohen-Or. Prompt-to-prompt im-

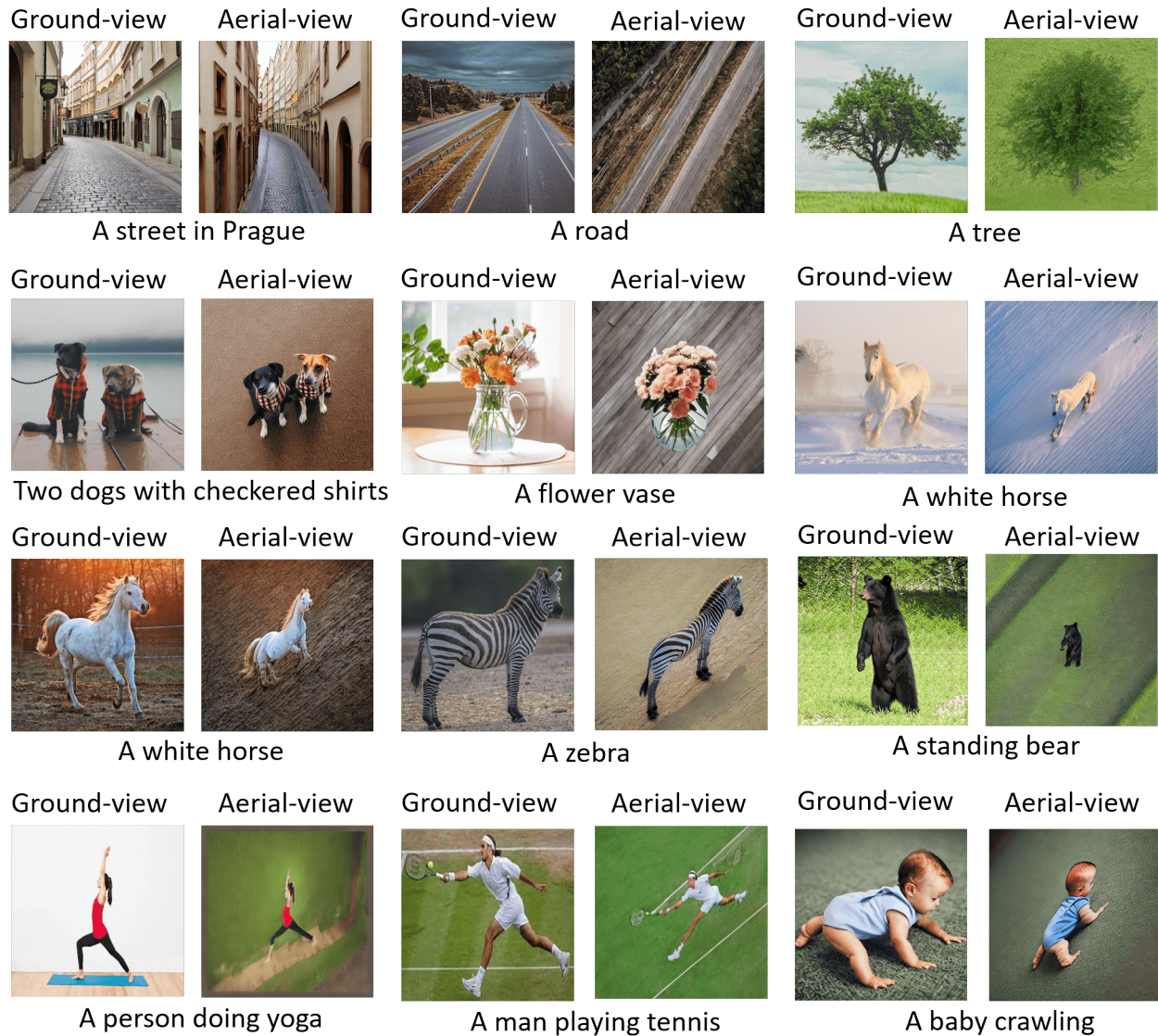


Figure 9: **Results.** We apply Aerial Diffusion on diverse images such as animals/ birds, natural scenes, human actions, indoor settings, etc and show that our method is able to generate high-quality high-fidelity aerial images.

- age editing with cross attention control. *arXiv preprint arXiv:2208.01626*, 2022. 2, 3, 4, 9
- [24] Jonathan Ho, Ajay Jain, and Pieter Abbeel. Denoising diffusion probabilistic models. *Advances in Neural Information Processing Systems*, 33:6840–6851, 2020. 4, 6, 7
- [25] MD Zakir Hossain, Ferdous Sohel, Mohd Fairuz Shiratuddin, and Hamid Laga. A comprehensive survey of deep learning for image captioning. *ACM Computing Surveys (CSUR)*, 51(6):1–36, 2019. 2, 3
- [26] Yuxin Hou, Arno Solin, and Juho Kannala. Novel view synthesis via depth-guided skip connections. In *Proceedings of the IEEE/CVF Winter Conference on Applications of Computer Vision*, pages 3119–3128, 2021. 3
- [27] Edward J Hu, Yelong Shen, Phillip Wallis, Zeyuan Allen-Zhu, Yuanzhi Li, Shean Wang, Lu Wang, and Weizhu Chen. Lora: Low-rank adaptation of large language models. *arXiv preprint arXiv:2106.09685*, 2021. 3
- [28] Xun Huang, Ming-Yu Liu, Serge Belongie, and Jan Kautz. Multimodal unsupervised image-to-image translation. In *Proceedings of the European conference on computer vision (ECCV)*, pages 172–189, 2018. 2
- [29] Phillip Isola, Jun-Yan Zhu, Tinghui Zhou, and Alexei A Efros. Image-to-image translation with conditional adversarial networks. In *Proceedings of the IEEE conference on computer vision and pattern recognition*, pages 1125–1134, 2017. 2
- [30] Nikita Jaipuria, Xianling Zhang, Rohan Bhasin, Mayar Arafa, Purnarjay Chakravarty, Shubham Shrivastava, Sagar Manglani,

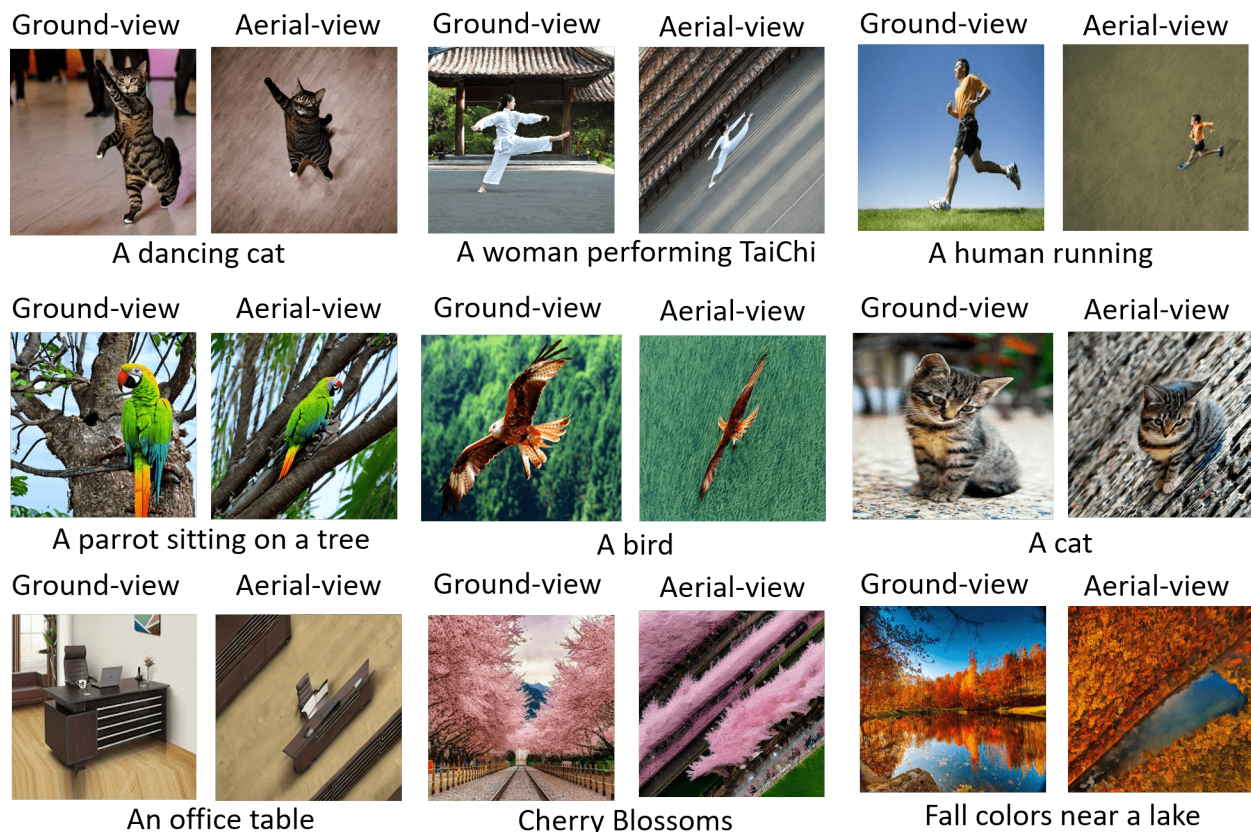


Figure 10: **Results.** We apply Aerial Diffusion on diverse images such as animals/ birds, natural scenes, human actions, indoor settings, etc and show that our method is able to generate high-quality high-fidelity aerial images.

- and Vidya N Murali. Deflating dataset bias using synthetic data augmentation. In *Proceedings of the IEEE/CVF Conference on Computer Vision and Pattern Recognition Workshops*, pages 772–773, 2020. 2
- [31] Yongcheng Jing, Yezhou Yang, Zunlei Feng, Jingwen Ye, Yizhou Yu, and Mingli Song. Neural style transfer: A review. *IEEE transactions on visualization and computer graphics*, 26(11):3365–3385, 2019. 2
- [32] Bahjat Kawar, Shiran Zada, Oran Lang, Omer Tov, Huiwen Chang, Tali Dekel, Inbar Mosseri, and Michal Irani. Imagic: Text-based real image editing with diffusion models. *arXiv preprint arXiv:2210.09276*, 2022. 2, 3, 4, 6, 8, 9, 15
- [33] Gwanghyun Kim, Taesung Kwon, and Jong Chul Ye. Diffusionclip: Text-guided diffusion models for robust image manipulation. In *Proceedings of the IEEE/CVF Conference on Computer Vision and Pattern Recognition*, pages 2426–2435, 2022. 3, 4
- [34] Divya Kothandaraman, Tianrui Guan, Xijun Wang, Shuowen Hu, Ming Lin, and Dinesh Manocha. Far: Fourier aerial video recognition. In *Computer Vision–ECCV 2022: 17th European Conference, Tel Aviv, Israel, October 23–27, 2022, Proceedings, Part XXXVII*, pages 657–676. Springer, 2022. 2
- [35] Rakesh Kumar, Harpreet Sawhney, Supun Samarasekera, Steve Hsu, Hai Tao, Yanlin Guo, Keith Hanna, Art Pope, Richard Wildes, David Hirvonen, et al. Aerial video surveillance and exploitation. *Proceedings of the IEEE*, 89(10):1518–1539, 2001. 1
- [36] Marc Levoy and Pat Hanrahan. Light field rendering. In *Proceedings of the 23rd annual conference on Computer graphics and interactive techniques*, pages 31–42, 1996. 3
- [37] Bowen Li, Xiaojuan Qi, Philip HS Torr, and Thomas Lukasiewicz. Image-to-image translation with text guidance. *arXiv preprint arXiv:2002.05235*, 2020. 3
- [38] Tianjiao Li, Jun Liu, Wei Zhang, Yun Ni, Wenqian Wang, and Zhiheng Li. Uav-human: A large benchmark for human behavior understanding with unmanned aerial vehicles. In *Proceedings of the IEEE/CVF conference on computer vision and pattern recognition*, pages 16266–16275, 2021. 1, 2
- [39] Jianxin Lin, Yingce Xia, Tao Qin, Zhibo Chen, and Tie-Yan Liu. Conditional image-to-image translation. In *Proceedings of the IEEE conference on computer vision and pattern recognition*, pages 5524–5532, 2018. 2
- [40] Gaowen Liu, Hugo Latapie, Ozkan Kilic, and Adam Lawrence. Parallel generative adversarial network for third-person to first-person image generation. In *Proceedings of*



Figure 13: **Results.** Based on the text description, Aerial Diffusion can generate aerial views with scene entities slightly different from the ground-view. The hallucination of background and unseen parts of the scene can also be controlled by text.

- what to change: A text-guided unsupervised image-to-image translation approach. In *Proceedings of the 28th ACM International Conference on Multimedia*, pages 1357–1365, 2020. **3**
- [45] Yuexin Ma, Tai Wang, Xuyang Bai, Huitong Yang, Yue-nan Hou, Yaming Wang, Yu Qiao, Ruigang Yang, Dinesh Manocha, and Xinge Zhu. Vision-centric bev perception: A survey. *arXiv preprint arXiv:2208.02797*, 2022. **3**
- [46] Chenlin Meng, Yutong He, Yang Song, Jiaming Song, Jiajun Wu, Jun-Yan Zhu, and Stefano Ermon. Sdedit: Guided image synthesis and editing with stochastic differential equations. In *International Conference on Learning Representations*, 2021. **15**
- [47] Mehdi Mirza and Simon Osindero. Conditional generative adversarial nets. *arXiv preprint arXiv:1411.1784*, 2014. **1**
- [48] Mathew Monfort, Alex Andonian, Bolei Zhou, Kandan Ramakrishnan, Sarah Adel Bargal, Tom Yan, Lisa Brown, Quanfu Fan, Dan Gutfreund, Carl Vondrick, et al. Moments in time dataset: one million videos for event understanding. *IEEE transactions on pattern analysis and machine intelligence*, 42(2):502–508, 2019. **1**
- [49] Amit More and Subhasis Chaudhuri. Deep learning based novel view synthesis. *arXiv preprint arXiv:2107.06812*, 2021. **3**
- [50] Alex Nichol, Prafulla Dhariwal, Aditya Ramesh, Pranav Shyam, Pamela Mishkin, Bob McGrew, Ilya Sutskever, and Mark Chen. Glide: Towards photorealistic image generation and editing with text-guided diffusion models. *arXiv preprint arXiv:2112.10741*, 2021. **1, 2, 9**
- [51] Yingxue Pang, Jianxin Lin, Tao Qin, and Zhibo Chen. Image-to-image translation: Methods and applications. *IEEE Transactions on Multimedia*, 24:3859–3881, 2021. **2**
- [52] Or Patashnik, Zongze Wu, Eli Shechtman, Daniel Cohen-Or, and Dani Lischinski. Styleclip: Text-driven manipulation of stylegan imagery. In *Proceedings of the IEEE/CVF International Conference on Computer Vision*, pages 2085–2094, 2021. **3**
- [53] Konpat Preechakul, Nattanat Chatthee, Suttisak Wizadwongsa, and Supasorn Suwajanakorn. Diffusion autoencoders: Toward a meaningful and decodable representation. In *Proceedings of the IEEE/CVF Conference on Computer Vision and Pattern Recognition*, pages 10619–10629, 2022. **2**
- [54] Alec Radford, Jong Wook Kim, Chris Hallacy, Aditya Ramesh, Gabriel Goh, Sandhini Agarwal, Girish Sastry, Amanda Askell, Pamela Mishkin, Jack Clark, et al. Learning transferable visual models from natural language supervision. In *International conference on machine learning*, pages 8748–8763. PMLR, 2021. **3**
- [55] Krishna Regmi and Ali Borji. Cross-view image synthesis using geometry-guided conditional gans. *Computer Vision and Image Understanding*, 187:102788, 2019. **1, 2, 3, 9**
- [56] Bin Ren, Hao Tang, and Nicu Sebe. Cascaded cross mlp-mixer gans for cross-view image translation. *arXiv preprint arXiv:2110.10183*, 2021. **3**

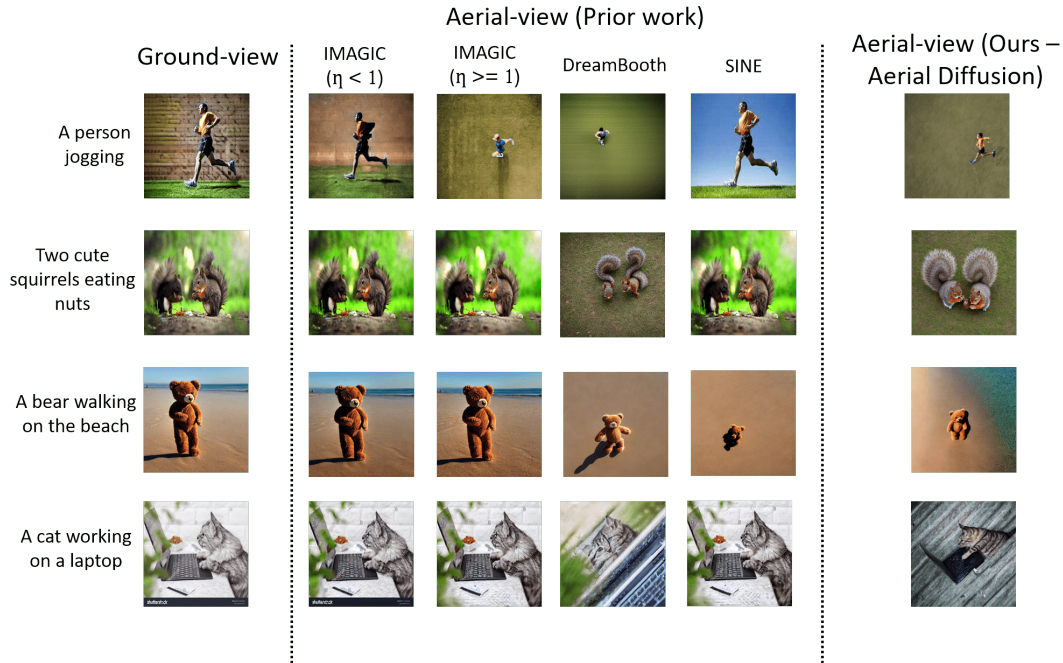


Figure 14: **State-of-the-art comparisons.** We compare with the state-of-the-art text-based image translation method, IMAGIC [32] (CVPR 2023). IMAGIC is unable to generate a high-fidelity **aerial-view** image. It merely reproduces the ground-view image, despite tuning all hyperparameters exhaustively. The hyperparameter η (in IMAGIC [32]) takes values between 0 and 1, and is unable to generate a high fidelity *aerial* image for any value of η . When η is increased to a value higher than 1, the model generates an aerial image but the fidelity with respect to the ground-view is completely lost. Other methods (contemporary/prior to IMAGIC [32] (CVPR 2023)) such as DDIB [70] (ICLR 2023), DreamBooth [59] (CVPR 2023), SINE [88] (CVPR 2023), SDEdit [46](ICLR 2022) and Text2LIVE [4](ECCV 2022) face the same issues. These are due to the challenges involved in ground-to-aerial translation described in Section 1 and Section 3.1 of our paper.

- [57] Bin Ren, Hao Tang, Yiming Wang, Xia Li, Wei Wang, and Nicu Sebe. Pi-trans: Parallel-convmlp and implicit-transformation based gan for cross-view image translation. *arXiv preprint arXiv:2207.04242*, 2022. 3
- [58] Robin Rombach, Andreas Blattmann, Dominik Lorenz, Patrick Esser, and Björn Ommer. High-resolution image synthesis with latent diffusion models. In *Proceedings of the IEEE/CVF Conference on Computer Vision and Pattern Recognition*, pages 10684–10695, 2022. 2, 5, 6, 7
- [59] Nataniel Ruiz, Yuanzhen Li, Varun Jampani, Yael Pritch, Michael Rubinstein, and Kfir Aberman. Dreambooth: Fine tuning text-to-image diffusion models for subject-driven generation. *arXiv preprint arXiv:2208.12242*, 2022. 3, 8, 9, 15
- [60] Chitwan Saharia, William Chan, Huiwen Chang, Chris Lee, Jonathan Ho, Tim Salimans, David Fleet, and Mohammad Norouzi. Palette: Image-to-image diffusion models. In *ACM SIGGRAPH 2022 Conference Proceedings*, pages 1–10, 2022. 2
- [61] Chitwan Saharia, Jonathan Ho, William Chan, Tim Salimans, David J Fleet, and Mohammad Norouzi. Image super-resolution via iterative refinement. *IEEE Transactions on Pattern Analysis and Machine Intelligence*, 2022. 2, 6
- [62] Hiroshi Sasaki, Chris G Willcocks, and Toby P Breckon. Unit-ddpm: Unpaired image translation with denoising diffusion probabilistic models. *arXiv preprint arXiv:2104.05358*, 2021. 2
- [63] Christoph Schuhmann, Romain Beaumont, Richard Vencu, Cade Gordon, Ross Wightman, Mehdi Cherti, Theo Coombes, Aarush Katta, Clayton Mullis, Mitchell Wortsman, et al. Laion-5b: An open large-scale dataset for training next generation image-text models. *arXiv preprint arXiv:2210.08402*, 2022. 3
- [64] Pourya Shamsolmoali, Masoumeh Zareapoor, Eric Granger, Huiyu Zhou, Ruili Wang, M Emre Celebi, and Jie Yang. Image synthesis with adversarial networks: A comprehensive survey and case studies. *Information Fusion*, 72:126–146, 2021. 2
- [65] Yujun Shen, Jinjin Gu, Xiaoou Tang, and Bolei Zhou. Interpreting the latent space of gans for semantic face editing. In *Proceedings of the IEEE/CVF conference on computer vision and pattern recognition*, pages 9243–9252, 2020. 3
- [66] Yan Shen, Meng Luo, Yun Chen, Xiaotao Shao, Zhongli Wang, Xiaoli Hao, and Ya-Li Hou. Cross-view image translation based on local and global information guidance. *IEEE Access*, 9:12955–12967, 2021. 3, 9

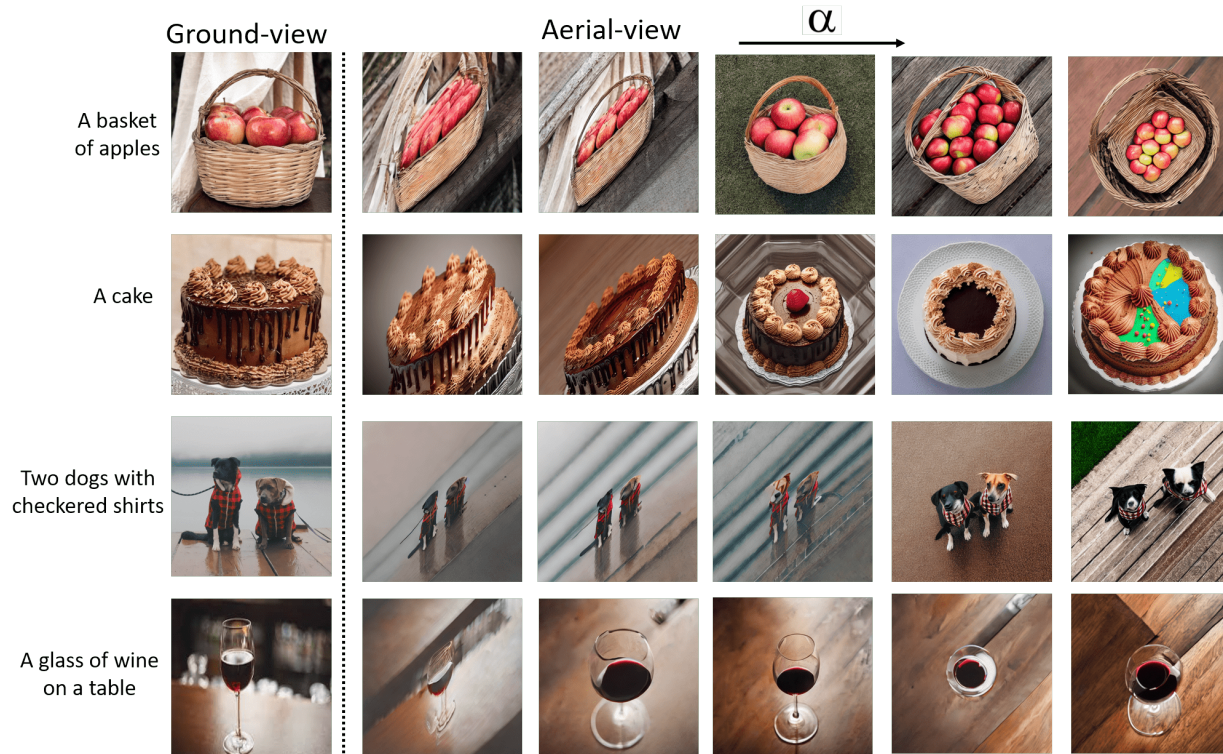


Figure 15: **Effect of α .** Low values of α generate images that are less aerial, high values of α generate low-fidelity images. A trade-off between the viewpoint and fidelity generates high-fidelity aerial images. The transformation, with α , is not smooth, reinforcing Postulate 2.

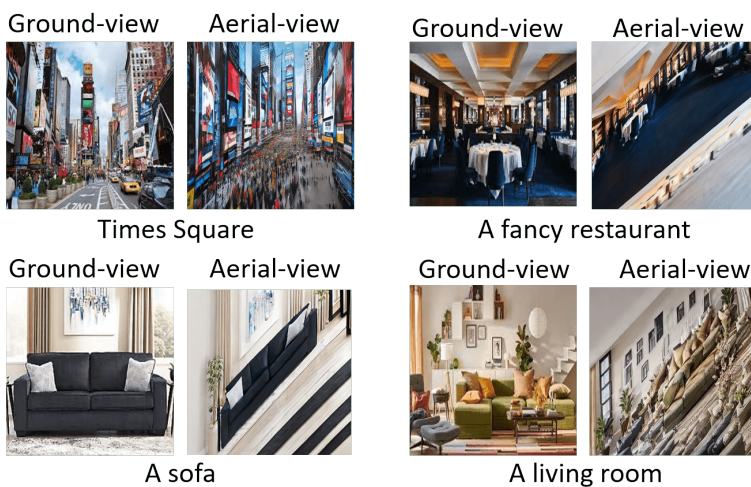


Figure 16: **Failure cases.** Our method is unable to generate high fidelity aerial views of scenes that have high complexity with multiple objects or scene entities, especially when the *text description* of the scene is *brief and inadequate*. This is a direction for future work.

[67] Yujiao Shi, Dylan Campbell, Xin Yu, and Hongdong Li. Geometry-guided street-view panorama synthesis from satellite imagery. *IEEE Transactions on Pattern Analysis and*

Machine Intelligence, 44(12):10009–10022, 2022. 3

[68] Gowthami Somepalli, Vasu Singla, Micah Goldblum, Jonas Geiping, and Tom Goldstein. Diffusion art or digital forgery?

- investigating data replication in diffusion models. *arXiv preprint arXiv:2212.03860*, 2022. 10
- [69] Jingwen Su, Boyan Xu, and Hujun Yin. A survey of deep learning approaches to image restoration. *Neurocomputing*, 487:46–65, 2022. 2
- [70] Xuan Su, Jiaming Song, Chenlin Meng, and Stefano Ermon. Dual diffusion implicit bridges for image-to-image translation. In *International Conference on Learning Representations*, 2022. 2, 15
- [71] Chen Sun, Austin Myers, Carl Vondrick, Kevin Murphy, and Cordelia Schmid. Videobert: A joint model for video and language representation learning. In *Proceedings of the IEEE/CVF international conference on computer vision*, pages 7464–7473, 2019. 2
- [72] Richard Szeliski. *Computer vision: algorithms and applications*. Springer Nature, 2022. 5
- [73] Hao Tang, Dan Xu, Nicu Sebe, Yanzhi Wang, Jason J Corso, and Yan Yan. Multi-channel attention selection gan with cascaded semantic guidance for cross-view image translation. In *Proceedings of the IEEE/CVF conference on computer vision and pattern recognition*, pages 2417–2426, 2019. 1, 2, 3
- [74] Aysim Toker, Qunjie Zhou, Maxim Maximov, and Laura Leal-Taixé. Coming down to earth: Satellite-to-street view synthesis for geo-localization. In *Proceedings of the IEEE/CVF Conference on Computer Vision and Pattern Recognition*, pages 6488–6497, 2021. 3, 9
- [75] Richard Tucker and Noah Snavely. Single-view view synthesis with multiplane images. In *Proceedings of the IEEE/CVF Conference on Computer Vision and Pattern Recognition*, pages 551–560, 2020. 3
- [76] Dani Valevski, Matan Kalman, Yossi Matias, and Yaniv Leviathan. Unitune: Text-driven image editing by fine tuning an image generation model on a single image. *arXiv preprint arXiv:2210.09477*, 2022. 3
- [77] Yael Vinker, Eliahu Horwitz, Nir Zabari, and Yedid Hoshen. Deep single image manipulation. *arXiv preprint arXiv:2007.01289*, 2020. 3
- [78] Tengfei Wang, Ting Zhang, Bo Zhang, Hao Ouyang, Dong Chen, Qifeng Chen, and Fang Wen. Pretraining is all you need for image-to-image translation. *arXiv preprint arXiv:2205.12952*, 2022. 2
- [79] Ting-Chun Wang, Ming-Yu Liu, Jun-Yan Zhu, Guilin Liu, Andrew Tao, Jan Kautz, and Bryan Catanzaro. Video-to-video synthesis. *arXiv preprint arXiv:1808.06601*, 2018. 2
- [80] Daniel Watson, William Chan, Ricardo Martin-Brualla, Jonathan Ho, Andrea Tagliasacchi, and Mohammad Norouzi. Novel view synthesis with diffusion models. *arXiv preprint arXiv:2210.04628*, 2022. 3
- [81] Olivia Wiles, Georgia Gkioxari, Richard Szeliski, and Justin Johnson. Synsin: End-to-end view synthesis from a single image. In *Proceedings of the IEEE/CVF Conference on Computer Vision and Pattern Recognition*, pages 7467–7477, 2020. 3
- [82] Songsong Wu, Hao Tang, Xiao-Yuan Jing, Haifeng Zhao, Jianjun Qian, Nicu Sebe, and Yan Yan. Cross-view panorama image synthesis. *IEEE Transactions on Multimedia*, 2022. 3
- [83] Xiaogang Xu, Ying-Cong Chen, and Jiaya Jia. View independent generative adversarial network for novel view synthesis. In *Proceedings of the IEEE/CVF international conference on computer vision*, pages 7791–7800, 2019. 3
- [84] Binxin Yang, Shuyang Gu, Bo Zhang, Ting Zhang, Xuejin Chen, Xiaoyan Sun, Dong Chen, and Fang Wen. Paint by example: Exemplar-based image editing with diffusion models. *arXiv preprint arXiv:2211.13227*, 2022. 2
- [85] Junjie Ye, Changhong Fu, Guangze Zheng, Danda Pani Paudel, and Guang Chen. Unsupervised domain adaptation for nighttime aerial tracking. In *Proceedings of the IEEE/CVF Conference on Computer Vision and Pattern Recognition*, pages 8896–8905, 2022. 1
- [86] Jihyeong Yoo and Qifeng Chen. Sinir: Efficient general image manipulation with single image reconstruction. In *International Conference on Machine Learning*, pages 12040–12050. PMLR, 2021. 3
- [87] Anny Yuniarti and Nanik Suciati. A review of deep learning techniques for 3d reconstruction of 2d images. In *2019 12th International Conference on Information & Communication Technology and System (ICTS)*, pages 327–331. IEEE, 2019. 3
- [88] Zhixing Zhang, Ligong Han, Arnab Ghosh, Dimitris Metaxas, and Jian Ren. Sine: Single image editing with text-to-image diffusion models. *arXiv preprint arXiv:2212.04489*, 2022. 2, 3, 6, 8, 9, 15
- [89] Yun Zhao, Yu Zhang, Zhan Gong, and Hong Zhu. Scene representation in bird’s-eye view from surrounding cameras with transformers. In *Proceedings of the IEEE/CVF Conference on Computer Vision and Pattern Recognition*, pages 4511–4519, 2022. 3
- [90] Jun-Yan Zhu, Taesung Park, Phillip Isola, and Alexei A Efros. Unpaired image-to-image translation using cycle-consistent adversarial networks. In *Proceedings of the IEEE international conference on computer vision*, pages 2223–2232, 2017. 2
- [91] Peiye Zhuang, Oluwasanmi Koyejo, and Alexander G Schwing. Enjoy your editing: Controllable gans for image editing via latent space navigation. *arXiv preprint arXiv:2102.01187*, 2021. 3